COMPARISON OF THE DYNAMIC RIVETING PROCESS OF A RIVET WITH AND WITHOUT A COMPENSATOR

Elzbieta Szymczyk, Grzegorz Slawinski, Jerzy Jachimowicz, Agnieszka Derewonko

Military University of Technology
Faculty of Mechanical Engineering
Department of Mechanics and Applied Computer Science
Kaliskiego 2, 00-908 Warsaw, Poland
tel.: +48 022 6839039, fax: +48 22 6839461
e-mail: eszymczyk@wat.edu.pl, gslawinski@wat.edu.pl

Abstract

The paper deals with the analysis of deformation of a rivet hole in a riveted joint after the manual dynamic riveting process. For many years, riveting remains a traditional and the most popular method of joining in aircraft structures. The residual stress and strain state appear at the rivet hole after the riveting process, which improves the joint's fatigue behaviour. The local finite element models are made with Patran. The rivet and sheets are described using eight-noded, three-dimensional brick elements. The riveting tools consist of four-noded, two-dimensional shell elements. Numerical FE simulations of the upsetting process are carried out using the Ls-Dyna code. The contact with friction is defined between the collaborating parts of the specimen. The results of simulations of the dynamic riveting process of a mushroom rivet with and without a compensator are compared in this paper. Hole deformation of the upper and lower sheet, squeezing force, as well as deformations of the rivet head are analysed. The influence of the compensator on strain and displacement states is studied. Simulation shows that some technological factors may have positive influence on the residual stress fields. Using the rivet with a compensator results in a better rivet hole filling capability. The rivet hole displacement in upper and lower sheets are at the same level. Paper also present manual dynamic riveting process of reverse and standard riveting procedure and model of riveted specimen.

Keywords: *riveted joint, mushroom rivet, FEM local model, deformation fields*

1. Introduction

Riveting is a traditional but still popular method of joining thin-walled parts of aircraft structures. It is used in large airliners, freight aircraft and in light fighter-trainers planes as well as in helicopters where riveting is the basic method of joining metal and composite components [1, 2]. The number of rivets is counted in millions and their weight may achieve a few tons. Therefore, fatigue resistance of the aircraft structure depends on thousands riveted joints, which are used to build it.

The methods of driving solid shank rivets can be classified in two types: static and dynamic. The static (squeeze) method is the most efficient one since it causes that all rivets are driven with uniform pressure and the rivet shank is sufficiently and regularly expanded to fill completely the rivet hole [3, 4]. Regrettably, the application of this method is limited.

The most common upsetting tool used in aircraft is the pneumatic riveter. Two methods of dynamic riveting can be used depending upon the location and accessibility of the part being jointed. In the former method, the manufactured head is driven with the set and a hammer while the shank's end is bucked with a suitable bucking bar, whereas in the latter one the shank's end is driven and the manufactured head is bucked. This method is called reverse riveting. The rivet driving requires a few hammer strokes. Their number should be limited to a minimum since too much hammering may change the crystalline structure of the rivet material. Two methods of dynamic riveting process are shown in Fig. 1.

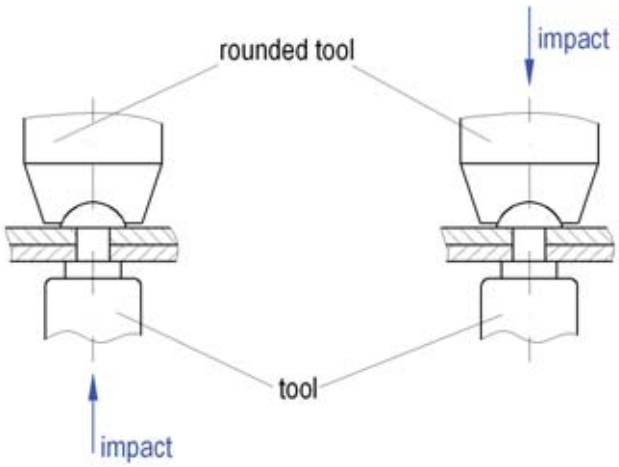

Fig. 1. Manual dynamic riveting process: a) reverse riveting procedure; b) standard riveting procedure

2. Numerical model

The analysis is carried out for the solid mushroom rivet (shank diameter d = 3.5 mm) joining two aluminium sheets (thickness 1.2 mm). The three-dimensional numerical model of the neighbourhood (10.5 mm wide) of a single rivet is considered (Fig. 2). Dimensions of the mushroom rivet are taken according to Russian standard [OST 1 34040-79] (head radius R = 4.2 mm, diameter D = 7 mm, height h = 1.88 mm). The radius R_p of the rounded tool surface is equal to 4.8 mm.

The models of rivet and sheets consist of eight-noded, isoparametric, three-dimensional brick elements (type Hex8) with tri-linear interpolation [5]. Materials used in riveted joints are subjected to high-strain deformation (plastic deformation). Tensile and compressive testing is required to determine mechanical property data like: Young's modulus of elasticity, yield strength and nonlinear behaviour of stress - strain curve above the yield stress level. Sheet material (2024-T3) is tested for standard flat specimen (in PN-91/H-04310 specification). Tensile and compressive tests are performed for the "rivet" sample.

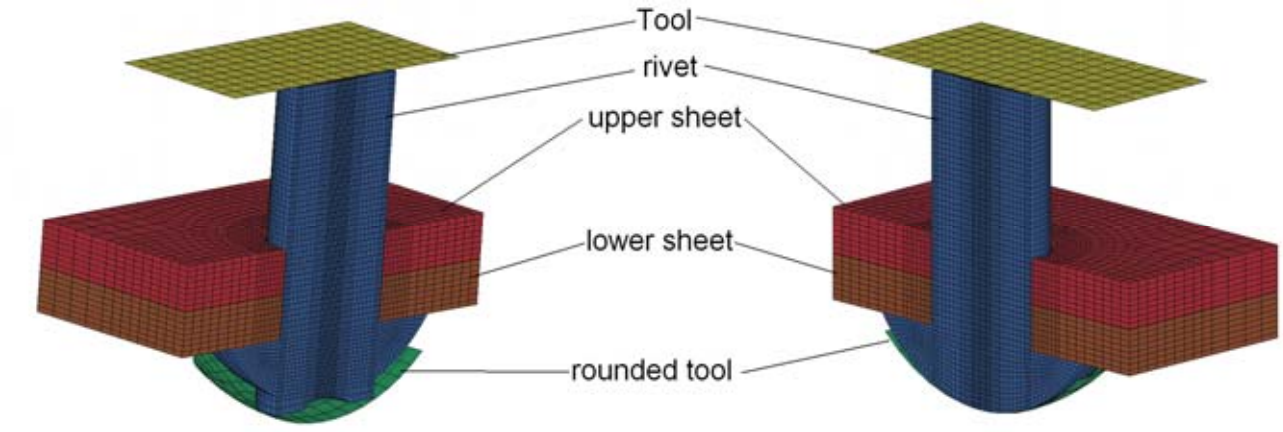

Fig. 2. Model of riveted specimen

Consequently elasto - plastic material models are considered. Multilinear material true stress – logarithmic strain curves [5] for sheet and rivet alloy are shown in Fig. 3. Material property data are presented in Tab. 1. The magnitude of the yield stress and tensile strength are obtained from uniaxial test. The yield stress for the multiaxial state is calculated using the von Misses yield criterion and it is based on the following formula:

$$\sigma_{equivalent} = \sqrt{\frac{3}{2}\sigma_{ij}^{d}\sigma_{ij}^{d}} = R_e\,, \tag{1}$$

where:
R_e – yield stress,
$\sigma_{ij}^{d} = \sigma_{ij} - \frac{1}{3}\sigma_{kk}\delta_{ij}$ – deviatoric Cauchy stress.

An explicit numerical procedure is used due to large geometrical and material non–linearities.

Table 1. Mechanical properies of aluminium alloys PA25 and 2024-T3

Aluminium alloy	Young's modulus [GPa]	Poisson's ratio ν	Yield stress [MPa]	Strenght [MPa]	Elongation [-]
PA25	71	0.33	318	488	0.14
2024-T3	68	0.3	374	460	0.16

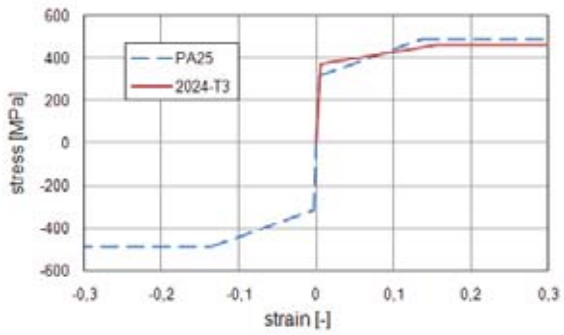

Fig. 3. Nonlinear stress–strain curves

The rounded and the flat rivet tools are described as rigid surfaces. The contact with friction is defined between the mating parts of the joint. The Coulomb friction model with friction coefficient $\mu = 0.2$ is used.

The outside edge of the sheets is constrained in normal direction. This model describes a part of the multi - riveted joint.

Two cases of the rivet geometry with and without a compensator (c1 and c2 respectively) are analysed.

Two load steps are considered: step I – upsetting the rivet, step II – unloading (removing the riveter). In case c2 the lower (rounded) tool is fixed and initial kinetic energy of 15 J is specified for the upper one (this is so called reverse riveting). The rivet with a compensator is driven according to standard (case c1s) and reverse (case c1r) riveting procedure. Three cases of the numerical simulation of the riveting process are shown in Fig. 4.

3. Numerical calculations

The numerical calculations are performed for three cases of upsetting (Fig. 4). Resultant dimensions (the height and diameter of the formed rivet head) are compared in Table 2.

Table 2. Formed rivet head dimensions

Case	**c1r**	**c1s**	**c2**
Head diameter D [mm]	5.12	5.12	5.31
Head height [mm]	2.17	2.13	2.26

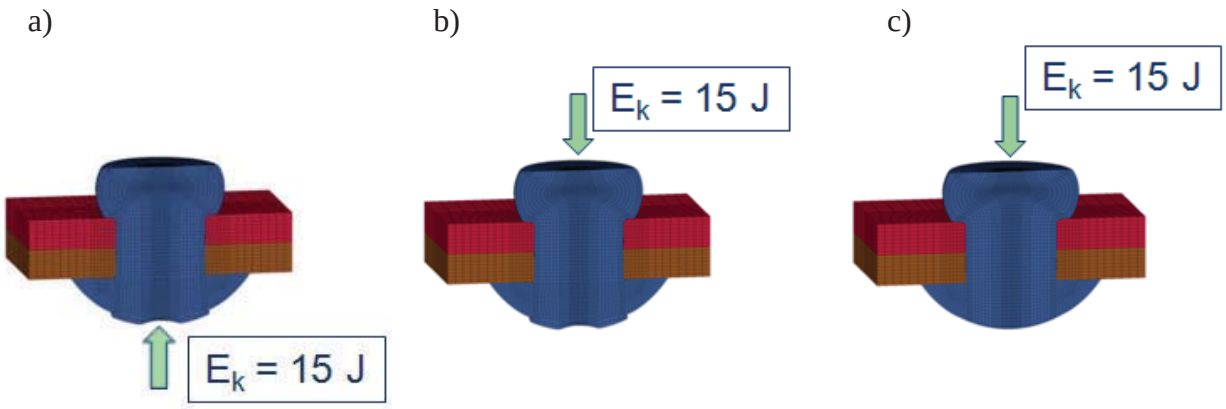

Fig. 4. Cases of numerical simulations: a) c1s; b) c1r; c) c2

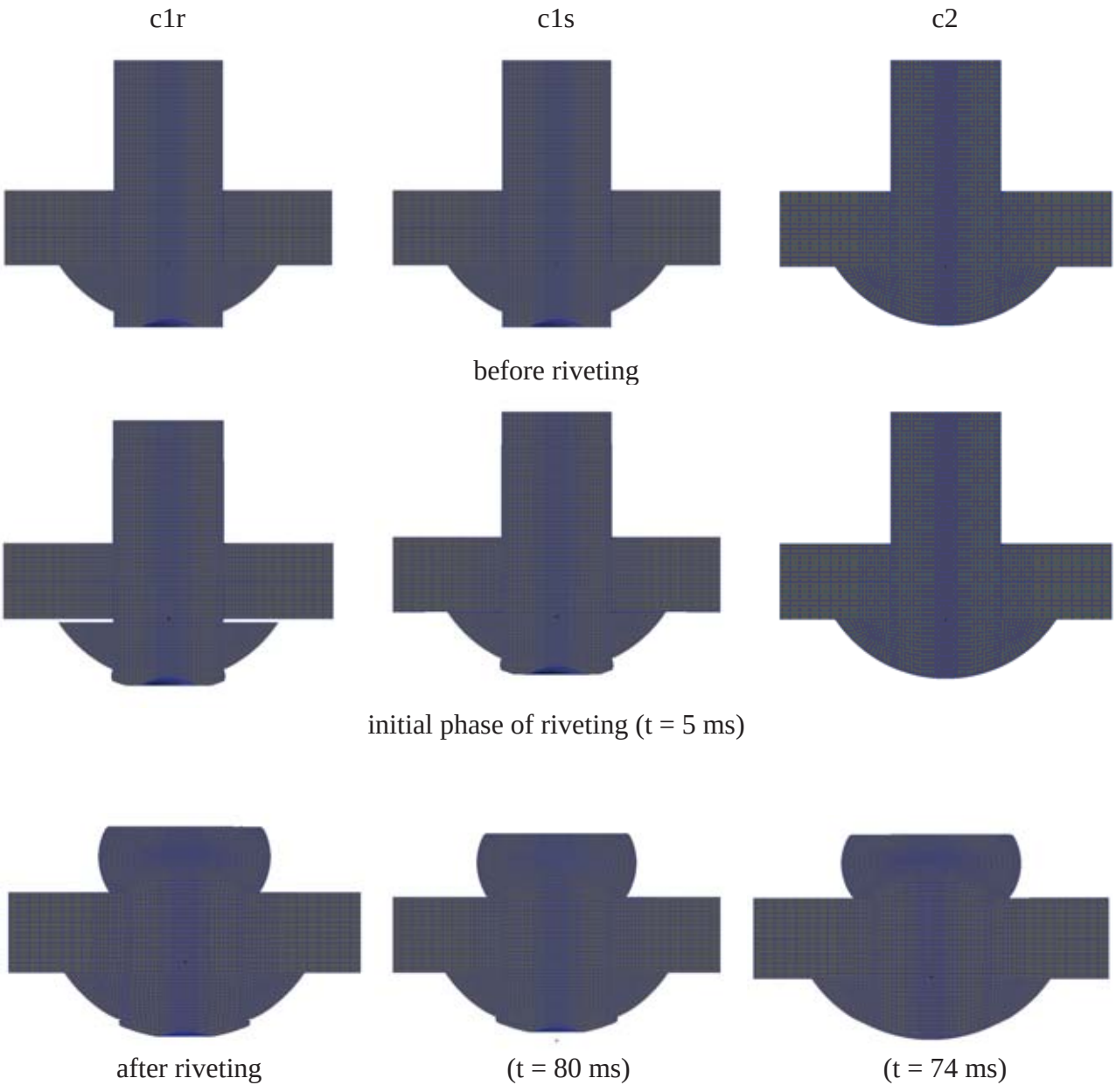

Fig. 5. Rivet deformation

The formed rivet diameter and the rivet hole filling capability depend on the rivet head height [6]. The nominal rivet head diameter ($D = 1.5d$) and the tolerance limits ($\pm 0.1d$) are specified in manufacturing instruction of riveting. Rivet deformations in each case for a selected time steps are presented in Fig. 5. The gap between the lower sheet and manufacturing rivet head appears after 5 ms for case c1r as a result of initial compression of a compensator.

The tool displacement vs. squeezing force during dynamic riveting process are presented in Fig. 6. In cases c1s and c1r results are similar and maximum value of squeezing force is equal 9 kN. In case c2, it is about 6% larger than in cases c1s and c1r.

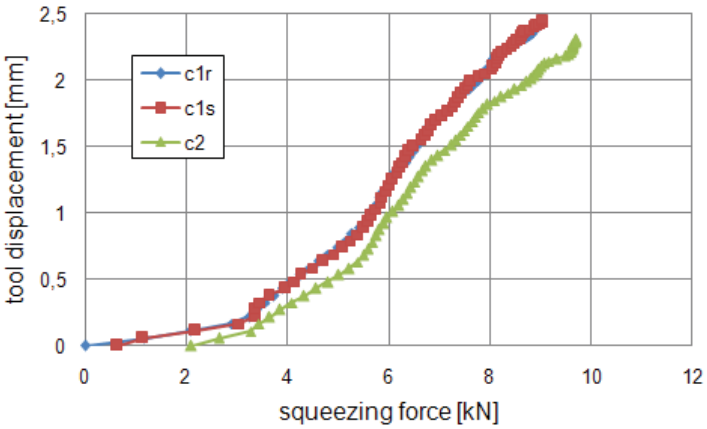

Fig. 6. Squeeze force during dynamic riveting process

Irreversible plastic deformations of sheet material around the rivet hole remain after the riveting process as a result of the rivet shank swelling in the hole.

The fields of the plastic strain in the upper and the lower sheet after unloading are presented in Fig. 7. An influence of the compensator causes uniform plastic strain distribution at the rivet hole after riveting process in both the upper and lower sheets. For rivets without compensator (c2), the hole in the upper sheet (from the side of the driven rivet head) is better filled with the rivet material than in the lower one.

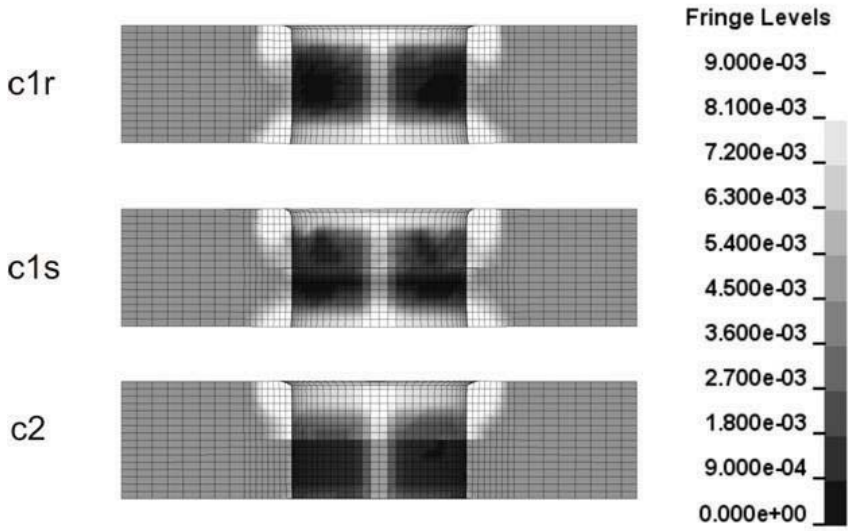

Fig. 7. Plastic strain fields in the upper and lower sheet

The fields of the radial displacement in the upper and lower sheet after II load step (unloading) are presented in Fig. 8. In case c1s and c1r displacements in sheets around the rivet hole are similar. In case c2, deformations around the rivet hole in the upper sheet are larger than in the

lower sheet. Extreme values of the radial displacement occur at the rivet hole for case c1s and are equal to 0.065 mm.

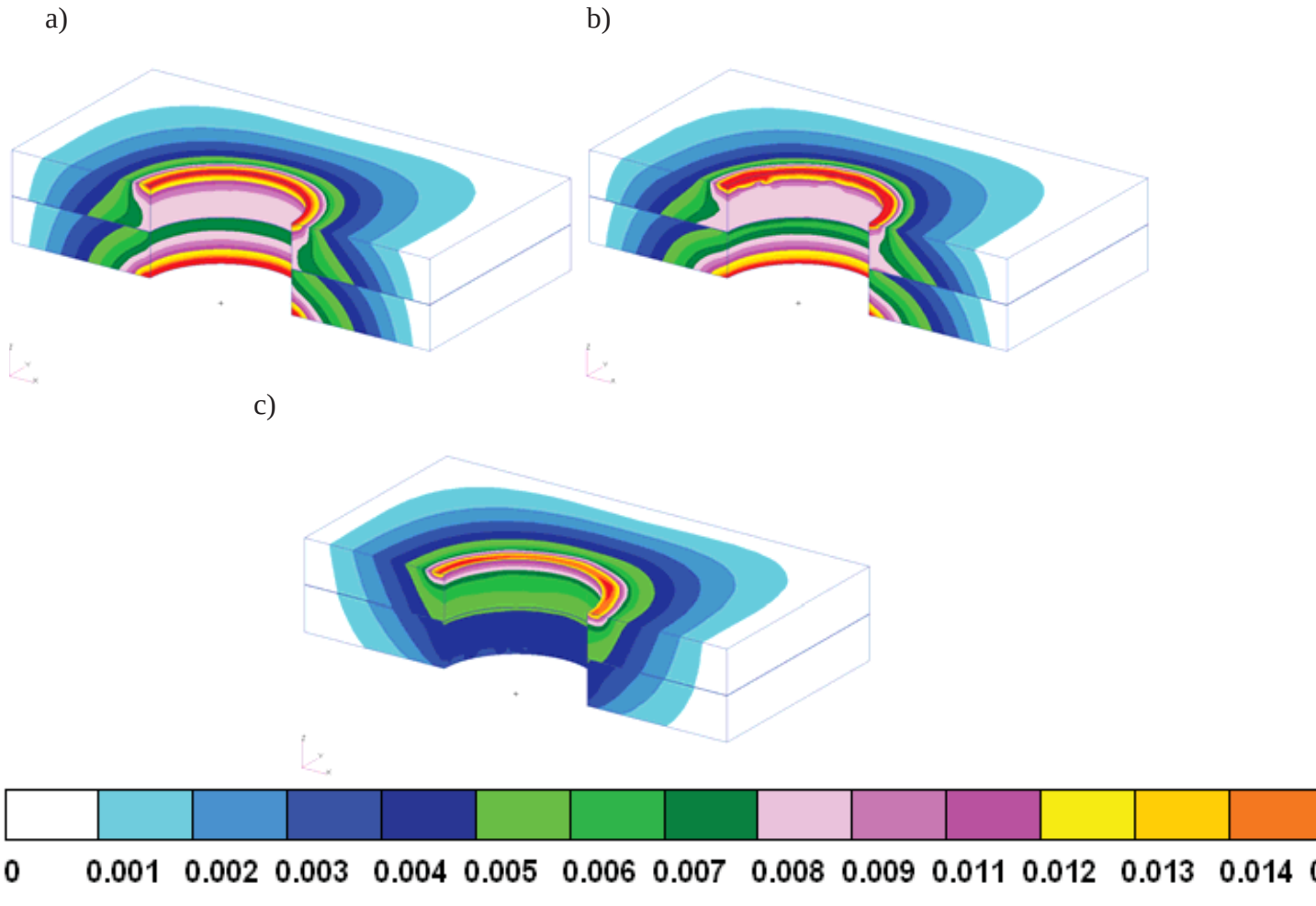

Fig. 8. Radial displacement fields in the upper and lower sheet: a) c1s; b) c1r; c) c2

The radial displacement in the middle surface of the upper and lower sheet versus radial distance from the rivet hole is shown in Fig. 9 and 10.

For the upper sheet after load step I (pressure), radial displacement values is not very sensitive to methods of driving.

For load step I (pressure) and II (unloading) curves are similar but after latter step the radial displacement values are about 24% lower than in the former one.

The rivet with compensator (c1r and c1s) has a significant influence on the radial displacement of the lower sheet (from the side of the shop rivet head). The radial displacement values for both cases (c1r and c1s) are similar while the maximum value of displacement is obtained for case c1r. However, for case c2 it is two times smaller than in cases c1r and c1s.

After load step II (unloading), the radial displacement values are about 30 % lower than in load step I (pressure).

Radial displacement versus axial distance of the rivet hole is presented in Fig. 11. After riveting the radial displacements of the rivet hole for case c1r and c1s are 0.011 mm on the average. Corresponding value in case c2 is two times smaller and is equal to 0.005 mm.

Changes of the height of the shop rivet head during the riveting process (case c1r, c1s and c2) are presented in Fig. 12. For each case this parameter decreases after upsetting process.

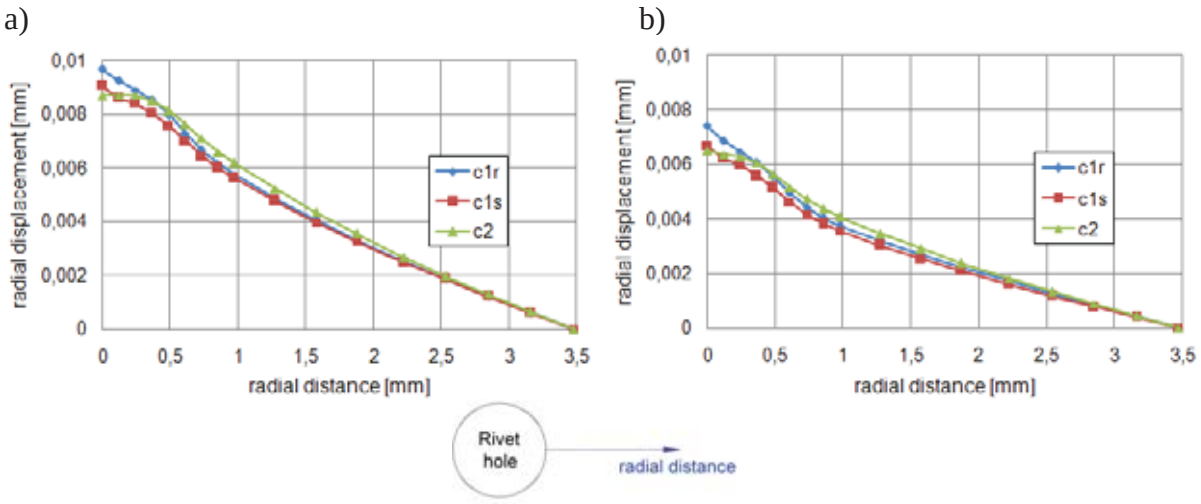

Fig. 9. Radial displacement values vs. radial distance in the upper sheet: a) pressure b) unloading

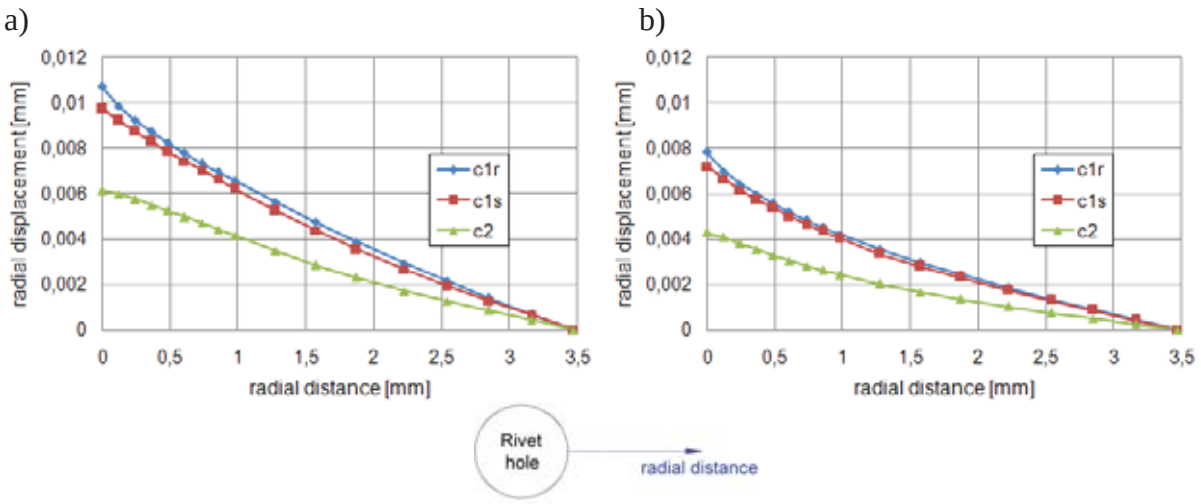

Fig. 10. Radial displacement values vs. radial distance in the lower sheet: a) pressure b) unloading

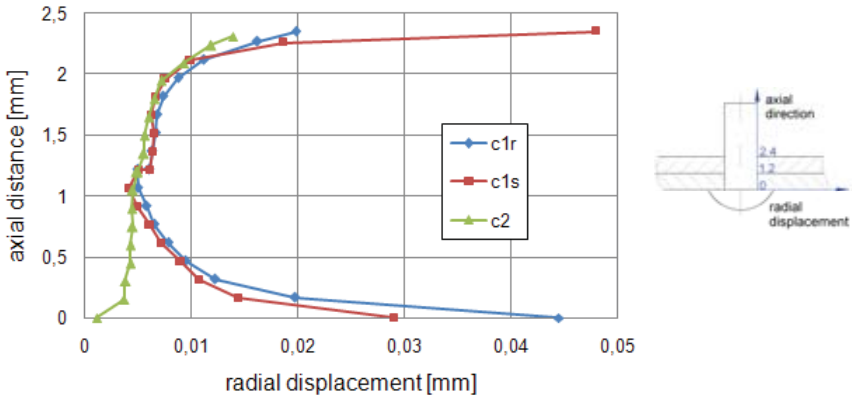

Fig. 11. Hole deformation vs. sheet axial distance

Maximum change of this component occurs for case c1s and is equal to 0.1 mm. A difference between head height before and after riveting process for case c2 is the smallest. It is a consequence of using the rivet without a compensator.

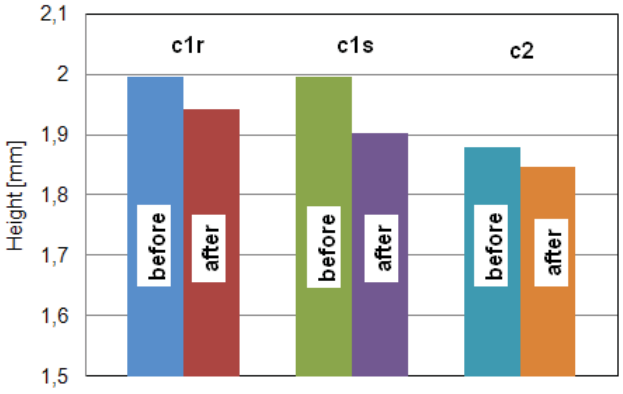

Fig. 12. Change of height of the shop rivet head during the riveting process

4. Conclusions

Some technological factors may have positive influence on the residual stress fields. With regard to the manufacturing process, an application of a compensator aiming at reducing the non-uniform stress distribution in the rivet hole is proposed and analysed. Using the rivet with a compensator results in a better rivet hole filling capability (better load transfer to the lower sheet). The rivet hole displacement in upper and lower sheets are at the same level.

Acknowledgements

This work was carried out with the financial support of Polish Ministry of Science and Higher Education under research project in the framework of the Eureka Initiative.

References

[1] Muller, R., *An experimental and numerical investigation on the fatigue behaviour of fuselage riveted lap joints*, Doctoral Dissertation, Delft University of Technology, Delft 1995.
[2] De Rijck, J., *Stress Analysis of Fatigue Cracks in Mechanically Fastened Joints*, Doctoral Dissertation, Delft University of Technology, Delft 2005.
[3] Szymczyk, E., Jachimowicz, J., Sławiński, G., Derewońko, A., *Numerical modelling and analysis of riveting process in aircraft structure*, (in polish), IX Międzynarodowa Konferencja Naukowa COMPUTER AIDED ENGINEERING, Szklarska Poręba 2008.
[4] Derewońko, A., Sławiński, G., Szymczyk E., Jachimowicz, J., *Modelowanie wybranych zagadnień dynamicznych*, IX Międzynarodowa Konferencja Naukowa COMPUTER AIDED ENGINEERING, Szklarska Poręba 2008.
[5] *Ls- Dyna Keyword User's Manual*, Version 971, Livermore Software Technology Corporation, May 2007.
[6] De Rijck, J., Homan, J. J., Schijve, J., Benedictus, R., *The driven rivet head dimensions as an indication of the fatigue performance of aircraft lap joints*, International Journal of Fatigue, 29, pp. 2208-2218, 2007.